www.gondwanags.org.in
Research Article

ISSN : 2455-1953
JGSR
Journal of Geosciences Research
Vol. 10, No.2, July, 2025, pp. 151-162

Assessment of Land Degradation Hotspots in Upper Savitri River Sub-Basin, Raigad District, India Using Geospatial Techniques and Analytic Hierarchy Process

Yogeshkumar Durugwar[1]*, Chandrakant Gurav[2], Swapnil Pekam[1] and Dhaval Kulkarni[1]

[1]*Department of Applied Geology, School of Earth Sciences, Punyashlok Ahilyadevi Holkar Solapur University, Solapur – 413255 (MS), India*
[2]*Department of Geology, Rajaram College, Kolhapur – 416004(MS), India*
*(*Corresponding Author, Email: yogesh.durugwar@gmail.com)*

Abstract

Due to rapid industrialization and physiography of the western ghat especially the region come into Maharashtra has faces land degradation problem. For understand the reasons of land degradation, Upper Savitri River area has been considered for the present work. Upper Savitri River is one of the main tributaries of Savitri River which originates in the eastern part of Poladpur Taluka (administrative boundary) of Raigad District, Maharashtra, India near the Sahyadri mountain. For this study, remote sensing, geographical information system (GIS) techniques and Analytic Hierarchy Process (AHP) modeling have adapted. For this work total nine thematic layers are considered *viz.,* geology, drainage density, aspect, slope, geomorphology, soil depth, rainfall, normalized difference vegetation index (NDVI) and land use land cover (LULC) have carried out. For study the normalized weight of each of this thematic layer, AHP modeling which is based on comparative matrix have been used. The results indicate that, rainfall and slope have the highest impact, accounting for 53% of the overall weightage. The land cover pattern and soil texture in this region, also point that a significant impact on lad degradation, contributing to 26% of the weightage. The remaining criteria collectively had a weightage of 22% in the analysis. Based on the intensity of land degradation and the extent of its impact, the Upper Savitri River area have classified into four categories i.e. very high, high, moderate and low vulnerability. Approximately 5.90% with 21.43 km^2 of the area is categorized as being under very high vulnerability, while around 74.59% with 271.04 km^2 is highly. Additionally, about 19.47% with 70.74 km^2 of the area is moderately vulnerable, and 0.04% with 0.14 km^2 is classified as low vulnerability. The research finding shows that the degradation of the land has mainly due to the intensity of rainfall in the region. These findings indicate that there is a pressing need to take measures to prevent further land degradation in the region.

Keywords: Analytic Hierarchy Process, Geospatial Techniques, Land Degradation, Savitri River Basin

Introduction

The sustainable development of human society depends on the land availability. However, in recent times, the issue of land degradation has emerged as a pressing concern, posing substantial challenges for human populations (Cowie *et al.*, 2018). According to Dobbs *et al.* (2017) the consequences of land degradation are evident in the decline of ecosystem functions, primarily manifested through the degradation of vegetation. Another study reveals that, anthropogenic disturbances and climate anomalies are the key drivers of land degradation, posing a significant and vulnerable threat to livelihoods and the sustainable development of societies (Fleskens and Sringer, 2014). Similarly, land degradation is influenced by a multitude of factors, including rainfall distribution, wind speed, slope, soil texture, as well as the type and coverage of ground vegetation (Maji *et al.*, 2010). Water-induced soil erosion, particularly during intense rainfall events and in areas with limited vegetation cover on exposed land surfaces, plays a dominant role in soil erosion processes (Aslam *et al.*, 2021).

Pal and Al-Tabbaa (2009) defined as 'soil erosivity refers to the vulnerability of soil to erosion caused by rainfall'. For accurate estimation of soil erosion, intra-seasonal time scales were followed (Grelle *et al.,* 2014). Consequently, this process leads to the detachment and transportation of soil particles via surface runoff (Schmidt *et al.,* 2016). Following the recommendation of Wischmeier and Smith (1978), rainfall maps were utilized to illustrate climatic variations, based on a minimum of 20 years of data as considered. Land degradation has been assessed and modeled based on multiple remote sensing datasets, as demonstrated in distinct as shown in Table 1. Land degradation vulnerability, which refers to in addition to rainfall, climatic dryness and poor soil quality, as well as agricultural intensification and deforestation determine an area's susceptibility to degradation and loss of productivity (Kosmas *et al.,* 2000). Managing natural resources and pursuing sustainable development require the modeling and assessment of land degradation vulnerability (Sandeep *et al.,* 2020).

(Received : 13 October 2024 ; Revised Form Accepted : 06 May 2025)
https://doi.org/10.56153/g19088-024-0234-78

Nevertheless, the central obstacle in this context pertains to the amalgamation of numerous parameters into a cohesive index, leveraging sophisticated methodologies and tools such as the Analytic Hierarchy Process (AHP) and Geographic Information System (GIS) (Sandeep *et al.*, 2020). Addressing this challenge would facilitate effective land management strategies aimed at mitigating land degradation and ensuring long-term sustainability. Remote sensing datasets and methodologies are progressively employed for the purpose of land degradation modeling and assessment, attributable to their capacity for swift and efficient evaluations across extensive geographical extents. Furthermore, they offer a dependable, cost-effective, and quantitatively robust source of consistent spatial information (Sandeep *et al.,* 2020).

Land degradation processes can be effectively assessed using remote sensing inputs, which are more cost-effective than conventional methods (Sujatha *et al.,* 2000; Bappa Das *et al.,* 2023). Land degradation assessments at regional and local scales have been improved by recent advancements in remote sensing and GIS technology (Reddy *et al.,* 2018). Different types of analyses can be performed using GIS technologies to extract spatial and temporal information from various types of land degradation datasets, enhancing the collection, storage, and manipulation of data (Essa, 2004). Land degradation is increasingly mapped using geospatial techniques because of their enormous potential for observing and executing land resources efficiently (Reddy *et al.,* 2018).

Earth observation satellites measure Normalized Difference Vegetation Index (NDVI) as a measure of the greenness and patterns of plant biomass based on the difference between greenness and brownness of vegetation (Forkel *et al.,* 2013). The investigation of spatiotemporal dynamics pertaining to alterations in vegetation holds utility in the evaluation and cartographic depiction of land degradation phenomena (Zhang *et al.*, 2008). Due to the ease of access to time-series different satellite image data and consistent NDVI digital datasets covering a wide area for at least two decades, in comparison with field-based studies, remote sensing is considered to be more robust. NDVI has been used as a biophysical indicator for assessing land degradation in humid and mountainous regions FAO, LADA (Nachtergaele *et al.,* 2009).

The present study area is a part of western ghat which is come under the state of Maharashtra. The southern part of Maharashtra especially Goa and Karnataka states also faces land degradation problem. Land degradation vulnerability map of west coast river basin (Mandovi River) Goa and Karnataka state shows high rainfall with high slopes and improper land use causing land degradation in the study area (Bappa *et al.*, 2023). Another study shown that, after heavy rainfall in short time induced creep movements have occurs in the talus deposits in Jotiba-Panhala hill range (a part of western ghat), such evidences give preliminary evidences of landslide predications in the regional level (Gurav *et al.,* 2017).

The complexity of land degradation processes makes AHP an ideal methodology to quantify land degradation since many parameters need to be considered when understanding the scenarios. An AHP technique compares attributes based on a scale of absolute judgments in order to determine how much one element dominates another on a given attribute (Sandeep *et al.,* 2020). Using GIS, various indicators can be integrated and assessed, spatial analysis and modeling can be performed (Sandeep *et al.*, 2020; Das *et al.,* 2023). The utilization of GIS based AHP assumes significance in the evaluation of land degradation vulnerability in regions characterized by non-uniform contributions of factors to land degradation, thereby exhibiting dissimilar magnitudes of influence (Sandeep *et al.,* 2020; Bappa Das *et al.,* 2023). The establishment of a land degradation vulnerability index necessitates the allocation of weights and ranks to input parameters and their respective subclasses. The veracity of the outcomes hinges upon the arrangement of rankings and weights accorded to these inputs and their subclasses. Experts exhibit a preference for the AHP due to its mathematical foundation, affording them objective and impartial information while quantifying intricate processes like land degradation (Sandeep *et al.,* 2020; Bappa Das *et al.,* 2023). For the evaluation and delineation of the extent of land degradation vulnerability, the integration of GIS and the AHP presents a viable approach (Sar *et al.,* 2015). By employing the AHP, attribute data derived from input thematic layers was transformed to produce a normalized weighted raster. Through the incorporation of remote sensing datasets, this research formulates and evaluates vulnerability to land degradation. AHP and GIS in the hot humid-per humid Eco-Region of the Western Ghat Upper Savitri Sub-basin region of west India.

Study Area

The Upper Savitri River, originating in eastern part of Poladpur Taluka of Raigad District, Maharashtra, India near the Sahyadri mountains, flows westward confluence with the Arabian Sea near Harihareshwar village. The study area (363.169 km²) covers 16.006% of the Savitri River and lies between 17°51' N to 18°05' N and longitudes 73°25' E to 73°39' E (Fig. 1). Elevation ranges from 3 m to 1316 m, with a relief of 1313 m. Geologically basin consists of Upper Cretaceous to Paleogene lava flows such as Purandargarh, Diveghat, and Karla formations (DRM, 2022). Soils, mainly Alfisols and Ultisols, are moderate to very deep, lateritic, and partially weathered basaltic, supporting vegetation productivity (NBSS&LUP, 1996).

Materials and Methods

For study hydro-morphometric characteristics of the basin, Survey of India (SoI) toposheet having map nos. 47F/8, 47F/12, 47G/1, and 47G/9 has been used. To maintain the accuracy and negate data gaps or any other misrepresentation, digital elevation has been used; The Cartosat-1 Digital Elevation Model (DEM) was procured from the National Remote Sensing Centre (NRSC), Hyderabad, India, at a spatial resolution of ten meters. It has been further used for preparation of slope and aspect maps of the study area.

In the present study area, land cover study has been carried out by using sentinel 2A satellite imagery having 10 m spatial resolution. For this, Supervised classification which is depends on the pixel of the stacked satellite imagery have carried out. For stacking, band 2, 3, 4 and 8 have used and then they are converted in to false color composition (FCC). This FCC has used for supervised classification, likewise NDVI also analyses. The rainfall data was taking from Indian Meteorological department (IMD) from 2016 to 2020 and it was converted in to Inverse Distance Weighting (IDW) grid data. The SoI toposheets having 1:50000 scale was used to prepare a drainage map and delineation of the basin area for study the drainage networks and the delineation of micro watersheds. The generation of a drainage density map involved the utilization of the line density functionality within the ARC GIS software. It was

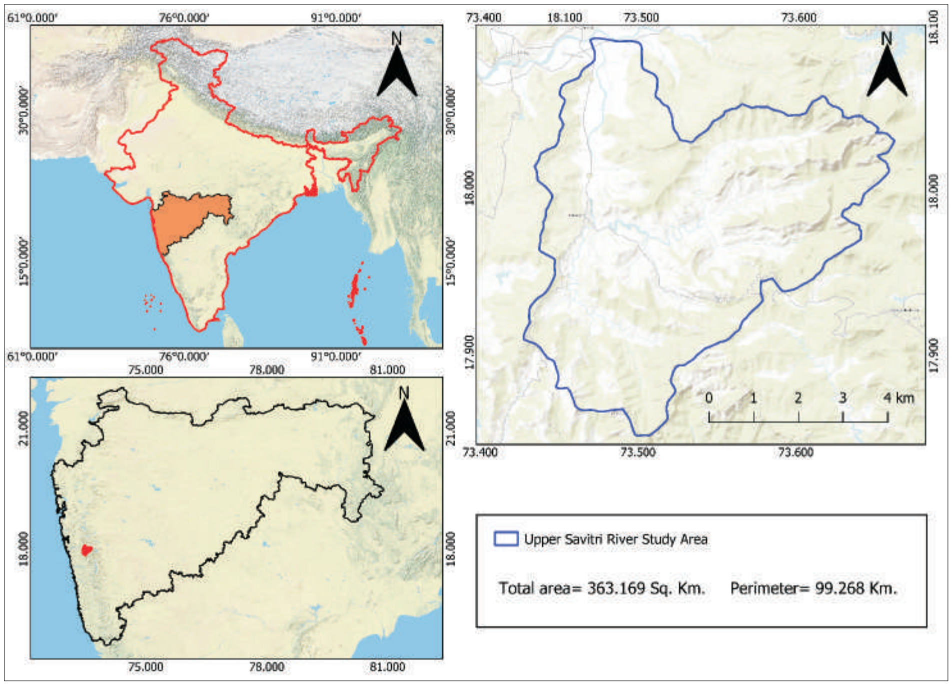

Fig.1. Location map of Upper Savitri River Sub-basin

further compared with the Cartosat-1 DEM extracted drainage network data to avoid data gaps. The analysis of flow chart given in Fig. 2.

Morphometric parameters such as linear, areal, and relief were extracted and analyzed using ArcGIS software covering the detail information of the thematic layers (Table 1). For the analysis of quantitative data and graphical representation, these were carried out in MS-Excel. Geomorphological and lithology study was undertaken using geomorphological and lithology layers using toposheet of the Survey of India (SoI) Bhukosh with 1:50000 scale. A total of five geomorphic units and three lithology units exists in the study area, soil data extracted from soil map of western part of Maharashtra acquired from National Bureau of Soil Survey (NBSS) soils bulletin (NBSS Publ. 54b) which has 1:500000 and these all units are used for soil degradation based on their normalized weight.

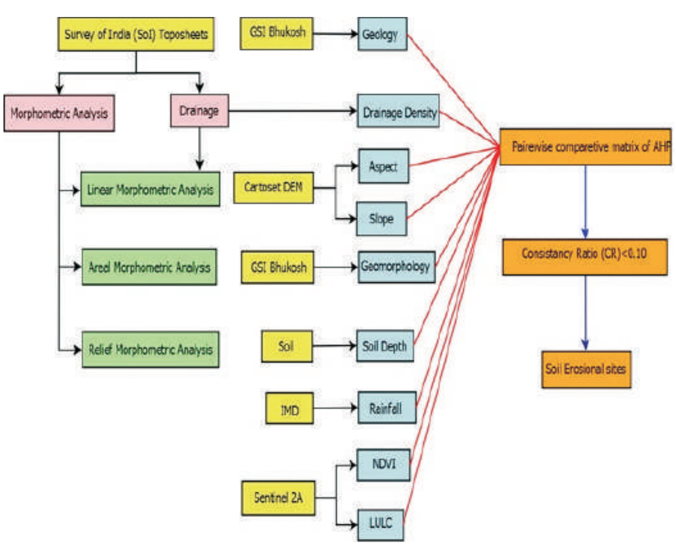

Fig.2. Flowchart of present methodology

Abbreviations

AHP: Analytic Hierarchy Process; CGWB: Central Ground Water Board; DEM: Digital Elevation Model; GIS: Geographical Information System; GSI: Geological Survey of India; IARI: Indian Agricultural Research Institute; IDW: Inverse Distance Weighting; IMD: Indian Meteorological Department; LDVI: Land Degradation Vulnerability Index; LULC: Land Use and Lands Cover; MCDM: multi-criteria decision-making; MSL: Mean Sea Level; NAAS: National Academy of Agricultural Sciences; NBSS: National Bureau of Soil Survey; NDVI: Normalized Difference Vegetation Index; NRSC: National Remote Sensing Centre; SOC: soil organic carbon; SoI: Survey of India; UHD: Ultra-high definition; USDA: United States Department of Agriculture; USGS: United States Geological Survey.

Table 1: Thematic layers used for land degradation analysis

Sl. No.	Parameters	Data type	Resolution/ Scale	Source
1.	Drainage/ Drainage density	Toposheet	1:50,000	Survey of India (SoI)
2.	Slope	Cartosat-1 DEM	10m × 10m	NRSC
3.	Aspect	Cartosat-1 DEM	10m × 10m	NRSC
4.	Rainfall	IMD gridded	10m × 10m	IMD Pune
5.	Geomorphology	Vector layer	1:50000	Survey of India (SoI) Bhukosh
6.	Geology	Raster	1:50000	Survey of India (SoI) Bhukosh
7.	Soil	Raster	1:500000	Survey of India
8.	Normalized Difference Vegetation Index (NDVI)	Sentinal 2A	10m × 10m	USGS Earth Explorer
9.	Land Use Land Cover (LULC)	Sentinal 2A	10m × 10m	USGS Earth Explorer

Results

Drainages/ Drainage Density

The drainage order was assigned for the streams and further morphometric parameters were calculated (Horten,1945; Fig. 3a). The metric of drainage density represents a significant determinant of the linear scale of landform components within fluvial eroded terrain (Horton 1945; Fig. 3b). The parameter in question quantifies the proximity of channel intervals and serves as a metric for characterizing the degree of landform incision and associated runoff capacity (Reddy, 2003). Areas characterized by low drainage density typically exhibit low resistant rock, highly permeable soil materials, densely covered vegetative having flat rolling topography. Conversely, regions displaying high drainage density are commonly found in areas with impermeable lithology, sparse vegetation, and mountainous terrain. Assessment of the study basin using the designated metric revealed a drainage density value of 3.33 km/km2, while the maximum drainage density value within the study region was determined to be 6.4 km/km2, indicating a correspondingly elevated potential for surface runoff. This information provides insights into the terrain attributes such as slope and lithology. Specifically, the Savitri basin exhibits a moderately to steeply sloping terrain, characterized by mountainous topography and a lithology comprising hard and rocky materials.

Slope

Upper Savitri River is originated from the Sahyadri Mountain which has maximum MSL of 4317 feet. Sub-basin slope maps were generated from Cartosat-1 DEM data, which presents the corresponding area-wise distributions and slope values (Fig. 3c; Table 2). Slope serves as a key parameter for characterizing the topographic conditions of a Savitri River Basin. While the discrepancy between maximum and minimum slope across sub-basins was relatively modest, a wide range of variation in slope distributions was observed across all gradient categories. Notably, the presence of high mean and range values suggests that the terrain of the basin is characterized by both steep and extensive topographic features. Slope is a critical factor that governs a range of hydrological processes, including stream network generation, runoff, and flooding. Water flow within a landscape is predominantly dictated by the direction of maximum slope. In regions characterized by steep topography, stream flow velocities are typically elevated, leading to a decrease in the time of concentration and an increase in erosion.

Additionally, high slope gradients are associated with reduced overland flow distances, resulting in a more rapid conveyance of water along channel pathways and leading to a rapid increase in hydrograph response. The influence of surface vegetation cover and channel gradient must also be considered in this context. Specifically, under uniform external conditions, dense

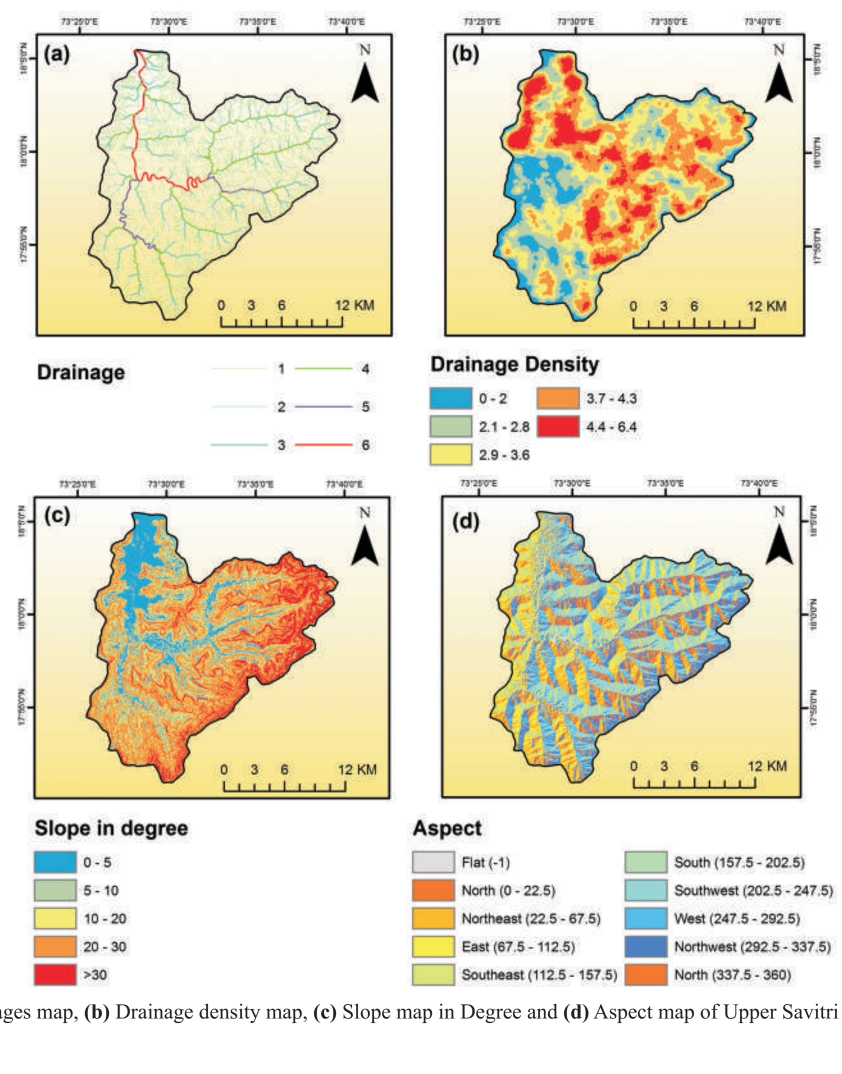

Fig.3. (a) Drainages map, **(b)** Drainage density map, **(c)** Slope map in Degree and **(d)** Aspect map of Upper Savitri River Sub-basin

Table 2: Slope analysis

Slope	Total area covered in km^2	Percentage
Gentle slope	119.00	32.78
Gentle to Moderate	129.0	35.54
Moderate to Steep	97.0	26.72
Very Steep	18.0	4.96
Total area	363.00	100
Relief Morphometry		
Maximum basin height (m)	1316	
Minimum basin height (m)	3	
Relief (m)	1313	
Relief ratio (km/km)	0.0486	

vegetation cover tends to reduce water flow and sediment transport, relative to areas with sparse vegetation (Samal *et al.*, 2014, 2015). Specifically, the minimum elevation was determined to be 03 meters, while the maximum elevation was recorded as 1316 meters for the entire sub-basin. The relief of a basin, which represents the vertical separation between its highest and lowest elevations, has significant implications for hydrological dynamics such as stream gradient, runoff patterns, and sediment transport capacity (Schumm and Hadley, 1961). The relief of the study area determined to be 1,313 meters. Schumm (1963) defined relief ratio (Rr) as a dimensionless measure of the height-to-length ratio of a basin, represented by the ratio of basin relief (R) to basin length (L). The calculated Rr value for the Savitri River Basin was 0.0486.

Aspect

The aspect map provides a comprehensive representation of the physical terrain, which is straightforward to interpret. Specifically, it characterizes the direction of slope face based on the classification of slope angle and aspect direction. The aspect map of the area given in Fig. 3(d). Aspect exerts a significant influence on precipitation patterns, solar radiation exposure, wind exposure, evaporation rates, and vegetation characteristics and density. In the western section of the sub-basin, slopes facing north, southeast, south, and southwest are prevalent. Aspect measured in the direction of slope in clockwise start off north at 0°. It back again on north with 360° rotation.

Rainfall

Rainfall exerts erosive forces on soil particles through the impact of raindrops, leading to detachment and separation of soil particles from the ground surface (Wischmeier and Smith, 1958). Rainfall erosivity, serving as an indicator of erosion potential, is influenced by various sub-factors including precipitation amount, spatial distribution, type, and other relevant characteristics (Mikoš *et al.*, 2006). Konkan costal belt of Maharashtra receives South-West (SW) monsoon through years, the rainy season started from the month of June to October. The rainfall data collected from Indian Meteorology Department (IMD) from 2016 to 2020 (Fig. 4) and represented in the IDW map (Fig. 6a). The climate of the basin is typical of the West Coast region and is characterized by abundant and regular seasonal precipitation, oppressive summer weather, and high humidity levels throughout the year (CGWB, 2013). Based on the analysis of long-term rainfall data, the normal annual precipitation in the study area ranges from 2197 mm to over 3360 mm in the plains and exceeds 5000 mm in the hills. The lowest precipitation values are observed in the northwest region around Uran (2197 mm), while the highest values are recorded around Mahad (3360 mm). The average rainfall over a 10-year period ranges from 2253 mm (Uran) to 7598 mm (Poladpur).

Geology

The upper Savitri River is situated in the Deccan Basaltic Province (DBP). Three types of lava flows, namely pahoehoe, compound, and simple, have been studied in the area (Cox *et al.*, 1985; Godbole *et al.*, 1996). The entire comes under Sahyadri Group, which is further classified into Mahabaleswar, Purandargarh, Diveghat, Karla and Indrayani formations (GSl) detail stratigraphy given in Table 3. The geological fieldwork was conducted travers from Polodpur to Talayachi Wadi. Most of the places including river channel show the compact basalt with columnar structure (Fig.5; Fig. 6b).

Geomorphology

Geomorphology is a scientific discipline that employs various methods to identify and analyze the landscape features of the Earth's surface and their relationship to underlying geological structures (Kale and Najaguru, 1988). Relict structures, which originate primarily from endogenetic processes, may be subject to modification by exogenetic processes such as weathering, erosion, and denudation. Present study area geomorphologically area classify into five classes (https://bhukosh.gsi.gov.in/) which are highly dissected structural upper plateau, moderately dissected structural upper plateau, highly dissected structural lower plateau, moderately dissected structural lower plateau, and pediment pediplain complex (Fig. 6c; Table 4).

Soil

The Konkan Coastal Belt (KCB) is dominated by basaltic soil

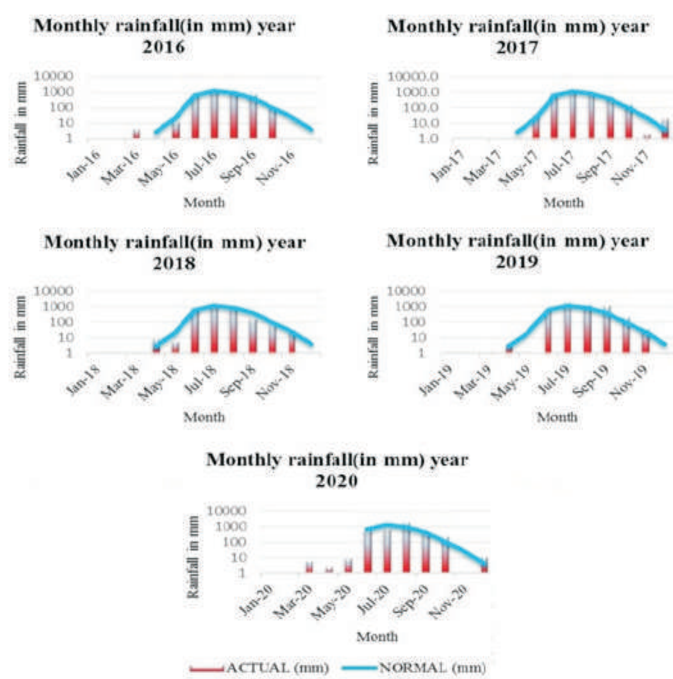

Fig. 4. Rainfall fluctuation graph during 2016 to 2020

Table 3: Stratigraphy of study area (*after* GSI)

Age	Super group	Group	Formation	Lithology	Lth Code
Cenozoic				Laterite	Czl
Upper Cretaceous to Palaeocene	Deccan Trap	Sahyadri	Mahabaleswar	Basalt Flow 1	dshmb 1
			Purandargarh	Basalt Flow 4 Basalt Flow 3 Basalt Flow 2-3 Basalt Flow 1-4 Basalt Flow 1-3	dshp 4 dshp 3 dshp 2-3 dshp 1-4 dshp 1-3
			Diveghat	Basalt Flow 4-5 Basalt Flow 3 Basalt Flow 2 Basalt Flow 1	dshd 4-5 dshd 3 dshd 2 dshd 1
			Karla	Basalt Flow 1	dshka 1
			Indrayani	Basalt Flow 1	dshi 1

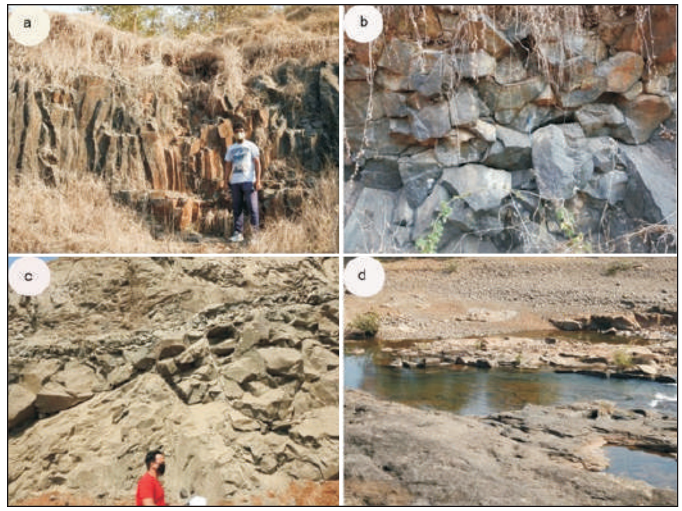

Fig. 5. Geological sites in Upper Savitri River (a) Columnar basalt at Poladpur Town, (b) Fractured and Jointed basalt along NH-64, (c) Compact basalt at Poladpur along NH-64, and (d) Amygdaloidal basalt along Upper Savitri Sub-basin

types. Basaltic soil is formed by the physic-chemical weathering process under conditions of heavy rainfall and high temperatures by the leaching of silica and enrichment of oxides of iron and aluminum (Bhattacharyya *et al.,* 1993, 1999). Such litho-types are known as lateritic soil, which is reddish to yellow in colour. Such soil contains iron, aluminum, titanium, and magnesium oxides as a major oxide (Mahoney, 1988). The soil taxonomy and extent of each mapped unit have been presented in Table 5, making use of the USDA soil classification system (Fig. 6d).

Normalized Difference Vegetation Index (NDVI)

To conduct a comprehensive land degradation study, it is necessary to possess a sound comprehension of vegetation factors, which cannot be directly derived from satellite-based band data. As a solution, the Normalized Difference Vegetation Index (NDVI) can be utilized to measure differences in vegetation. To evaluate the area acquired by vegetation, NDVI profiles were generated for various land cover classes. For this, 2019, 2020, and 2021 pre- and post-monsoon season Sentinel 2A satellite imagery containing band 4 and band 8 have processed under GIS software (Fig.7). Pre and post monsoon area are calculated and given in Table 6. Raster mapping via satellite band rationing is a crucial element to obtain reliable results given below.

$$NDVI= ((NIR-RED))/ ((NIR+RED))$$

During normal operation, the satellite system acquires data every five days (Cai *et al.,* 2019; Castaldi *et al.,* 2019; Yang *et al.,* 2020). In particular, studies have found that S2 offers a sufficient spatial resolution for accurately estimating vegetation heterogeneity and soil organic carbon (SOC) on both a local and a regional scale (Castaldi *et al.,* 2019). It has been found that the

Table 4: Geomorphology of the study area

Geomorphic units	Lithology	Relief	Area (Km^2)	Inference
Highly dissected structural upper plateau	5 Pahoehoe Flows Compound Pahoehoe Flows, Simple 20 Flows	65	229.6	A plateau area that has been highly eroded such that the relief is sharp.
Moderately dissected structural upper plateau	5 Pahoehoe Flows Compound Pahoehoe Flows, Simple 20 Flows	52	4.91	A plateau area that has been moderately eroded such that the relief is sharp.
Highly dissected structural lower plateau	5 Pahoehoe Flows Simple 20 Flows	30	0.27	Moderate slope weathered rock formation
Moderately dissected structural lower plateau	5 Pahoehoe Flows Simple 20 Flows	39	22.64	Moderate to gentle slope with weathered rock formation
Pediment pediplain complex	5 Pahoehoe Flows Simple 20 Flows	45	98.72	Gentle slope with sedimentation
Alluvial plane covered by Water body	Unrecognized	--	7.02	Very gentle slope with sedimentation

Table 5: National Bureau of Soil Survey (NBSS) soils bulletin (NBSS Publ. 54b)

Mapping units	Description	Taxonomy	Area (Km^2)
6	Slightly deep, well drained, loamy soils	Fine-loamy, mixed, isohyperthermic, Udic Rhodustalfs	0.28
31	Moderately deep, well drained, clayey soils	Clayey-skeletal, mixed isohy- perthermic, Typic Ustropepts	103.65
34	Shallow, well drained, loamy soils	Loamy-skeletal, mixed, isohyper- thermic, Lithic Ustorthents	163.62
46	Very deep, well drained, loamy soils	Fine-loamy, mixed, lsohyperther mic, Udic Rhodustalfs	11.27
47	Moderately shallow, well drained, loamy soils	Fine-loamy, mixed, isohyperther- mic, Udic Rhodustalfs	4.43
61	Very shallow, well drained, loamy soils	Loamy, mixed, isohyperthermic, Lithic Ustorthents	41.01
77	Very shallow, somewhat excessively drained, clayey soils	Clayey, mixed, isohyperthermic, Lithic Ustorthents	38.68

bands of the visible spectrum that are most conducive to NDVI mapping are the blue (490 nm), red (560 nm), and green (490 nm) bands (Ben-Dor *et al.,* 1997; Nocita *et al.,* 2015; Castaldi *et al.,* 2019). In addition, S2 incorporates two broad bands within this spectral range centered at 1610 and 2190 nm, the region of shortwave infrared (SWIR) that exhibits associations with specific chemical bonds. Accordingly, Sentinel-2 satellites provide spectral bands that correspond to those essential for estimation of NDVI (Castaldi *et al.,* 2019).

Land Use Land Cover (LULC)

According to Survey of India (SOI-Bhukosh), Land Use Land Cover (LULC) represents a specific type of classification practice. It is necessary to conduct land-based observations in order to calculate this factor. Using satellite-based LULC, land degradation and soil conservation practice can be divided into various zones. In the present study area, the regions of barren land, build-up, forest areas, agriculture field and water body were classified and distribution is shown in Fig. 8.

AHP is a versatile and effective decision-making technique that can assist in setting priorities and making informed decisions in scenarios where both quantitative and qualitative aspects of decisions are taken into account. Within the framework of AHP modeling, the initial step involves the formulation of a decision-making hierarchy, succeeded by the creation of matrices for the comparison of potential pairs to establish weights and ascertain consistency ratios. In the present investigation, the allocation of priority or weight to individual parameters and their respective subcategories necessitated the construction of a pairwise

Table 6: Pre and Post monsoon NDVI

	2019		2020		2021	
	Pre	Post	Pre	Post	Pre	Post
Barren land	2.0	36.0	0.7	0.5	0.3	26.0
Dense vegetation	8.6	87.8	28.5	126.6	9.6	122.9
Moderate vegetation	80.1	135.0	94.1	172.2	98.9	146.2
Sparse vegetation	271.1	102.6	238.7	62.9	253.1	65.6
Water body	1.4	1.7	1.3	1.0	1.2	2.4

comparison matrix. This matrix facilitated the assessment of parameter and subcategory precedence through the application of the Saaty pairwise comparison scale, encompassing values spanning from 1 to 9. The ensuing representation portrays the constructed pairwise comparison matrix:

$$M = \begin{bmatrix} 1 & a12 & a13 & \ldots & a1n \\ a21 & 1 & a22 & \ldots & a2n \\ a31 & a31 & 1 & \ldots & \ldots \\ \ldots & \ldots & \ldots & \ldots & \ldots \end{bmatrix}$$

Following is the formula for determining weightage:

a_{ij} = Assigning weight to attributes i / Assigning weight to attributes j

The pairwise comparison matrix assigns weights to individual parameters across a numerical continuum ranging from 1 to 9. In instances where the significance of two parameters (i and j) is equivalent, the corresponding matrix element is designated a value of 1. Throughout this procedure, the eigenvector elements, normalized for the context, are subjected to weighting contingent

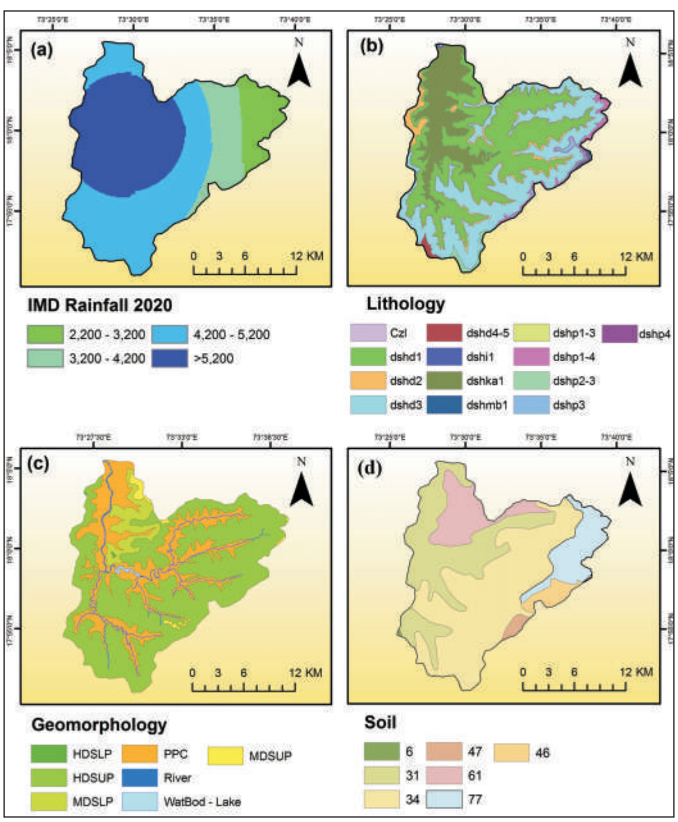

Fig. 6. (a) IMD Rainfall distribution, **(b)** Geology map, **(c)** Geomorphology map and **(d)** Soil map of Upper Savitri River Sub-basin

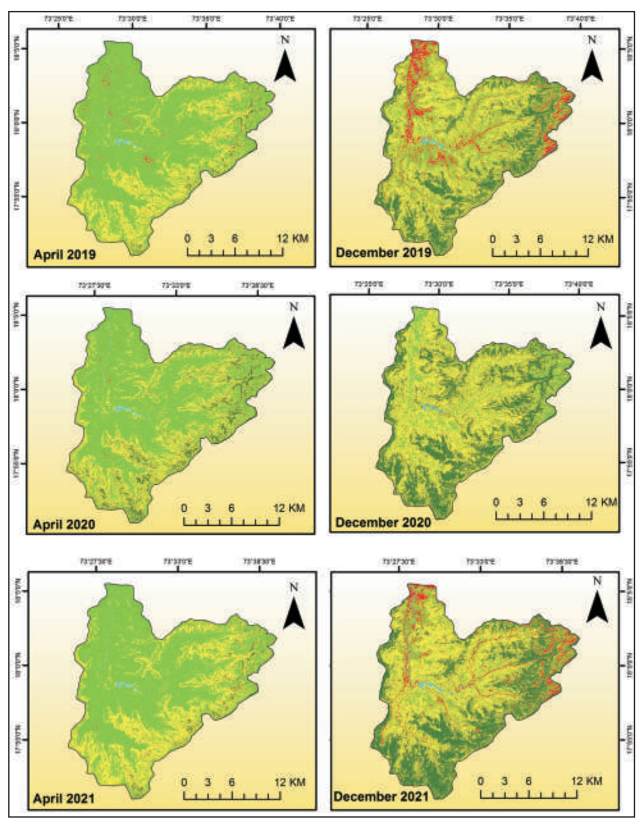

Fig.7. Normalized Difference Vegetation Index (NDVI) map of Upper Savitri River Sub-basin

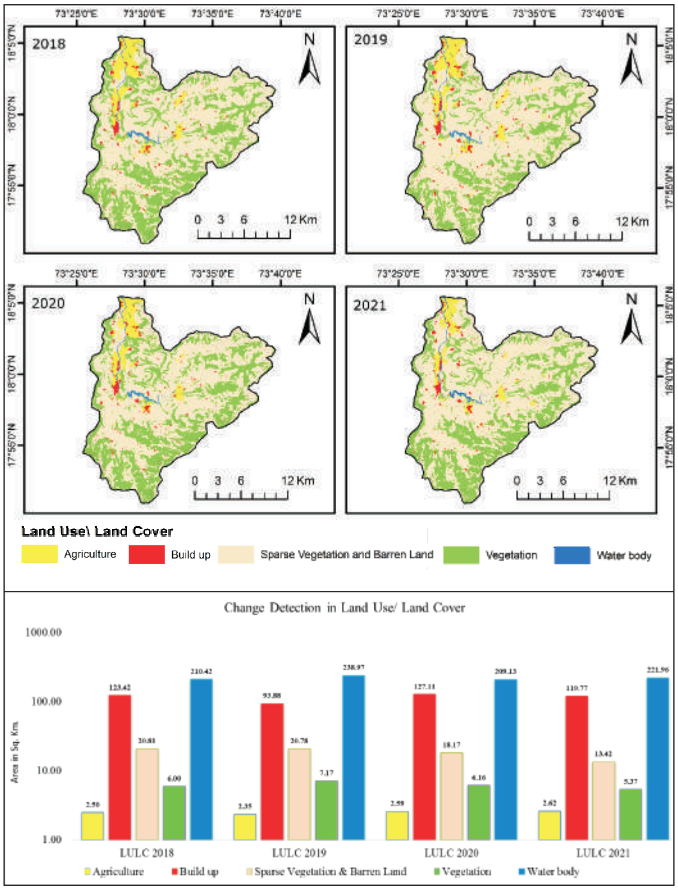

Fig.8. Land Use Land Cover map of Upper Savitri River Sub-basin

upon the criteria or sub-criteria, subsequently undergoing evaluation vis-à-vis the alternatives.

Weight Assignments in AHP

The AHP method has shown potential in identifying soil erosion and land degradation zones in multi-criteria decision-making (MCDM). Over the past two decades, the MCDM approach has emerged as a useful tool in river basin management, as it enhances the decision-making process by providing structure, auditability, transparency, and rigor (Arulbalaji *et al.,* 2019). Shekhar and Pandey (2014) demonstrated that AHP is an effective and efficient method for managing spatial data with the aid of GIS. Various researchers have utilized the AHP method to determine the weights of thematic layers and their classes, enabling the identification of land degradation zones.

The current study assessed the impact of nine individual parameters on land degradation, including Aspect, Geomorphology, Drainage density, Geology, NDVI, rainfall, soil, LULC, and slope. Each causative factor has a distinct level of influence on land degradation scenarios; therefore, understanding and determining the influence of each factor is crucial. To achieve this, a pairwise comparison matrix was generated, and developed a rating scale (Saaty,1980; Saaty and Vargas, 2012) and used to compare each factor with one another (Table 7). A weight was assigned to each criterion based on its significance in relation to other criteria. For example, rainfall and slope are direct indicators of degradation in a given area and were assigned greater weight than other criteria in the comparison scale. Similarly, the LULC and Soil map (Sm) of the study area were found to be erratic, significantly impacting land productivity, and thus were assigned higher values but less than rainfall and slope. The influence of each criterion on land degradation was subsequently analyzed to determine its weight. The results of the pairwise comparison matrix and the factor weights are presented in Table 8.

Table 7: Saaty pairwise comparison scale (Saaty, 1980)

Scale	Importance
1	Equal importance
2	Weak
3	Moderate importance
4	Importance plus
5	Strong importance
6	Strong plus
7	Very strong importance
8	Very, very strong
9	Extreme importance

Obtaining the weight of the parameters considered in the study, it is essential to conduct a consistency check. The consistency ratio (CR) is a measure of the reliability of the comparison and is obtained by dividing the consistency index (CI) of the matrix by the random index (RI). The expressed as a value ranging from 0 to 1.

$$CR = \frac{C21}{R1}$$

According to the formula below, CI is the consistency index of the normalized matrix

$$C1 = \frac{\lambda max - n}{n - 1}$$

In the AHP, the reliability of the pairwise comparisons made in the decision-making process is assessed by the consistency ratio (CR). The CR is obtained by dividing the consistency index (CI) of the matrix by the random index (RI), where CI is calculated as the difference between the largest eigenvalue (λ_{max}) and the number of criteria (n), divided by n-1. The RI is the average coherence index of randomly generated matrices with the same number of elements as the original matrix. In this study, since the number of elements in the matrix is 9, the RI was found to be 1.45, as shown in Table 9.

If the CR value is less than 0.1, the consistency value is considered acceptable, while a revised judgment is required if the CR value exceeds 0.1. In the current study, the CR value of the main parameters was found to be 0.067. This indicates a high level of consistency in the pairwise comparison. Finally, the obtained

Table 8: Pare Wise Comparative Matrix

TL	As	Ge	Dd	Geo	NDVI	Sm	LULC	Sl	Ra
As	1	2	3	4	5	6	7	8	9
Ge	0.50	1	2	3	4	5	6	7	8
Dd	0.33	0.50	1	2	3	4	5	6	7
Geo	0.25	0.33	0.50	1	2	3	4	5	6
NDVI	0.20	0.25	0.33	0.50	1	2	3	4	5
Sm	0.17	0.20	0.25	0.33	0.50	1	2	3	4
LULC	0.14	0.17	0.20	0.25	0.33	0.50	1	2	3
Sl	0.13	0.14	0.17	0.20	0.25	0.33	0.5	1	2
Ra	0.11	0.13	0.14	0.17	0.20	0.25	0.33	0.5	1
	2.83	4.72	7.59	11.45	16.28	22.08	28.83	36.50	45.00

Where: Rainfall (Ra), Slope (Sl), Land Use and Land Cover (LULC), Soil map (Sm), Normalized Difference Vegetation Index (NDVI), Geology (Geo), Drainage density (Dd), Geomorphology (Ge), Aspect (As) weights of each parameter were incorporated into reclassified input layers in GIS to generate the final output raster of land degradation vulnerability.

Generating Land Degradation Vulnerability Maps by Using GIS

To generate a quantitative and spatial representation of land degradation vulnerability, the GIS-based modeling approach utilized AHP-based weights assigned to the input parameters and calculate normalized pare wise comparative matrix (Table 9). The highest weight was assigned to Rainfall (Ra), followed by Slope (Sl), Land Use and Land Cover (LULC), Soil map (Sm), Normalized Difference Vegetation Index (NDVI), Geology (Geo), Drainage density (Dd), Geomorphology (Ge), and Aspect (As). The land degradation vulnerability index was computed using the following equation:

$$LDVI = Ra + Sl + LULC + Sm + NDVI + Geo + Dd + Ge + As$$

The LDVI formula was applied to produce a land degradation vulnerability raster (Fig. 9), which was then classified into four categories: low, moderate, high, and very high. Random validation was performed on moderate, high, and very high LDVI classes using ultra-high definition (UHD) true-color Google Earth images of the growing season of 2022 at identified sites. The methodology used in this study is illustrated in the flow chart.

Table 9: Normalized Pare Wise Comparative Matrix

TL	Ra	Sl	LULC	Sm	NDVI	Geo	Dd	Ge	As	Weight	Lamda
Ra	0.35	0.42	0.40	0.35	0.31	0.27	0.24	0.22	0.20	0.31	9.71
Sl	0.18	0.21	0.26	0.26	0.25	0.23	0.21	0.19	0.18	0.22	9.78
LULC	0.12	0.11	0.13	0.17	0.18	0.18	0.17	0.16	0.16	0.15	9.72
Sm	0.09	0.07	0.07	0.09	0.12	0.14	0.14	0.14	0.13	0.11	9.55
NDVI	0.07	0.05	0.04	0.04	0.06	0.09	0.10	0.11	0.11	0.08	9.34
Geo	0.06	0.04	0.03	0.03	0.03	0.05	0.07	0.08	0.09	0.05	9.17
Dd	0.05	0.04	0.03	0.02	0.02	0.02	0.03	0.05	0.07	0.04	9.08
Ge	0.04	0.03	0.02	0.02	0.02	0.02	0.02	0.03	0.04	0.03	9.10
As	0.04	0.03	0.02	0.01	0.01	0.01	0.01	0.01	0.02	0.02	9.22

Where: Rainfall (Ra), Slope (Sl), Land Use and Land Cover (LULC), Soil map (Sm), Normalized Difference Vegetation Index (NDVI), Geology (Geo), Drainage density (Dd), Geomorphology (Ge), Aspect (As), Consistency index (CI) = 0.10, coherence index (RI) = 1.45, Consistency ratio (CR) = 0.067

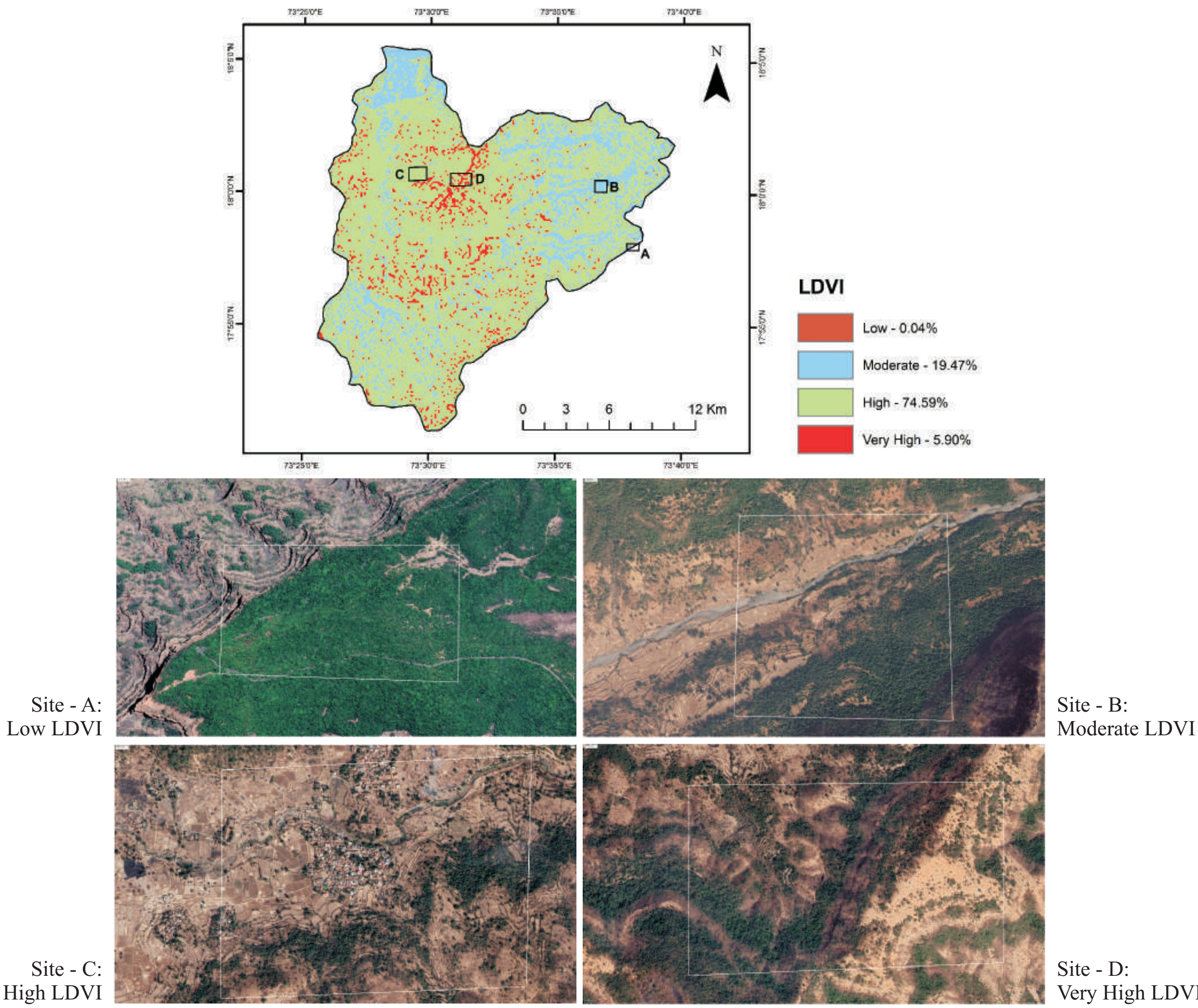

Fig. 9. Land Degradation Vulnerability Index (LDVI) for the Upper Savitri River Sub-basin

Discussions

The land degradation study of upper Savitri has carried out with the help of nine thematic layers such as geology, drainage density, aspect, slope, geomorphology, soil depth, rainfall, NDVI and land cover analysis have carried out.

The rainfall study revealing that the eastern and central parts of Raigad district of Poladpur taluka receive relatively low rainfall (< 2200 mm), while the western parts receive rainfall exceeding 5000 mm. Rainfall is one of the important climatic factors as far as land degradation is concerned because of heavy rainfall on sparsely vegetated lands results in runoff and soil erosion, washing away valuable topsoil and leaving the land barren and prone to degradation (Bappa *et al.,* 2023). Slope, derived from Cartosat-1 (10 m), indicates that the eastern and central parts of the region, which are at the foot hill of the Sahyadri range, are associated with slopes greater than 40°-50°, whereas lower slopes of >25° are confined to the flat terrain in western parts of the study area. For study the land degradations, many researchers have given the higher weightage to the slope (Mzuri *et al.*, 2021; Torabi Haghighi *et al.*, 2021; Abuzaid *et al.*, 2021). Vegetation cover over the land and pattern of the vegetation significantly important because of it reduces the impact of rainfall over land thereby considerably reducing land degradation (Mzuri *et al.*, 2021). Mean land use and land cover (LULC) data from 2018 to 2021 illustrate that built-up areas are increasing year on year, with decreasing dense and sparse vegetation. The soil study shows that deep soils occur in eastern region, it was consisting of fine-loamy soil, while the western parts consist of clayey soil. The northern and southern plains of the region were dominated by loamy soils, which are composed of a relatively balanced mixture of sand, silt, and clay particles, making them susceptible to both water and wind erosion processes.

Loamy soils have good water-holding capacity but can become waterlogged during heavy rainfall events, leading to soil saturation and ultimately erosion by water. Furthermore, loamy soils have poor structure and can easily become compacted, reducing infiltration rates and increasing surface runoff, which can lead to erosion by both water and wind. The fine-textured nature of loamy soils also makes them more vulnerable to wind erosion, as the smaller particles are more easily lifted and transported by wind. Predominantly, the study locale is encompassed by loamy soils, with a notable concentration observed in the central and northern sectors, rendering these areas more susceptible to water-induced soil erosion. Somewhat elevated and exceedingly drained soils typify the uplands and hilly terrains of the investigation region. Spatial analysis of the temporal mean NDVI spanning the interval 2019 to 2021 reveals that regions in the northwestern, western, and central sectors exhibit diminished NDVI values (ranging from 0.15 to 0.25), indicative of limited vegetative growth. Conversely, the northeastern, eastern, and southeastern parts of the study vicinity, particularly the Eastern Ghats, manifest elevated NDVI values (> 0.55), underscoring robust vegetative coverage.

The study developed a Land Degradation Vulnerability Index (LDVI) for the Upper Savitri sub-watershed area, using an AHP and GIS-based modeling approach. The LDVI values were categorized into four classes, namely low, moderate, high, and very high as shown in Table 10. The mean LDVI value for the study area was found to be 0.314, with a range of 0.04 to 0.590. The analysis revealed that only 0.04% of the study area, i.e., 0.14 sq. km., was under very low LDVI, which was mainly observed in the eastern parts of the region characterized by flat topography, high vegetative cover, and adequate rainfall ranging from 2200 to 3500 mm. The moderate LDVI class covered 19.47% (70.74 sq. km.) of the study area, mainly in the northeast, southwest, and northwest parts of the region, characterized by high and very high vegetative cover, high rainfall ranging from 4400 to 5500 mm, simple 20 basaltic flow, and shallow well-drained loamy soils. The high LDVI class covered the majority of the study area, accounting for 74.59% (271.03 sq. km.), and was mainly observed in the western and eastern parts of the region, characterized by moderate to low vegetative cover, rainfall ranging from 4400 to 5900 mm, simple 20 lava flows with moderately deep, well-drained, clayey soils, and shallow, well-drained, loamy soils. This region mainly comprised sparse to moderate vegetation and agricultural land. The very high LDVI class covered 5.9% (21.43 sq. km.) of the study area, mainly in the northern, southern, and central parts of the region, characterized by very less to moderate vegetation, very high to moderate rainfall (< 5900, 4400–5200 mm), and moderately dissected plateau. The study also highlighted that 19.47% (70.74 sq. km.) and 74.59% (271.03 sq. km.) of the study area were under moderate and high vulnerability of land degradation, respectively, mainly in the central, northeast, and southwest parts of the region, which were aggravated by adequate and erratic rainfall, slope, NDVI, and unfavorable soil conditions.

Table 10: LDVI at Upper Savitri River

LDVI	Area (km^2)	In %
Low	0.14	0.04
Moderate	70.74	19.47
High	271.04	74.59
Very high	21.43	5.90

Conclusions

The combined evaluation of terrain indicators and climate variations in the study area facilitated the identification of influential mechanisms affecting diverse land utility types. For LDVI study integrated rainfall, slope, aspect, NDVI, LULC, geology, geomorphology characteristics, drainage density and pedological parameters using AHP and GIS to assess land degradation vulnerability. The targeted objective was accomplished through the integrated analysis of GIS and Remote Sensing (RS) techniques, complemented by statistical analysis and AHP decision-making, which yielded robust outcomes. The results showed that a significant area of the study area is under moderate, high, and very high vulnerability to land degradation, with the highest vulnerability found central and northern region. The study demonstrates the potential of AHP and GIS-based modeling in assessing land degradation vulnerability, and the results can be used to suggest appropriate soil conservation and management measures for sustainable land resource management in the region. The results were validated using ultra-high-definition true color Google Earth images.

Authors' Contributions

YD: Writing – Review and Editing, Writing – Original Draft, Methodology, Investigation, Data Curation, Conceptualization. **CG:** Methodology, Investigation, Data Curation. **SP:** Investigation, Data Curation. **DK:** Methodology, Investigation, Conceptualization.

Conflict of Interest

The authors declare that they have no known competing financial interests or personal relationships that could have appeared to influence the work reported in this paper.

Data and Resources

Data will be made available on request. Sentinal 2A data are freely provided by USGS Earth Explorer Agency and can be downloaded from the USGS Earth Explorer site (https://earthexplorer.usgs.gov/). Toposheet acquire from Survey of India. Cartosat-1 DEM acquire from NRSC, Hyderabad. Rainfall data is freely provided by IMD Pune (https://imdpune.gov.in/). Geomorphology and Geology data are freely provided Survey of India (SoI) Bhukosh (https://bhukosh.gsi.gov.in/).

Acknowledgments

The authors express their gratitude to the National Remote Sensing Centre (NRSC) Hyderabad for generously supplying high-resolution data and offering valuable guidance. They also extend their appreciation to the Rajiv Gandhi Science and Technology Commission, an initiative of the Government of Maharashtra, for granting project approval and providing financial support for research, analysis, and assistance having grant numbers PAHSUS/RGST/File-01/933.

References

Abuzaid, A.S., Abdel Rahman, M.A.E., Fadl, M.E. and Scopa, A. (2021). Land degradation vulnerability mapping in a newly-reclaimed desert oasis in a hyper-arid agro-ecosystem using AHP and geospatial techniques. Agronomy, v.11, pp.1426. https:// doi. org/ 10. 3390/ agronomy11 071426

Arulbalaji, P., Padmalal, D. and Sreelash, K. (2019). GIS and AHP Techniques Based Delineation of Groundwater Potential Zones: a case study from Southern Western Ghats, India. Scientif. Rep., v.9(1). https://doi.org/10.1038/s41598-019-38567-x

Aslam, B., Maqsoom, A., Alaloul, W. S., Musarat, M. A., Jabbar, T. and Zafar, A. (2021). Soil erosion susceptibility mapping using a GIS-based multi-criteria decision approach: Case of district Chitral, Pakistan. Ain Shams Engineer. Jour., v.12(2), pp.1637–1649. https://doi.org/10.1016/j.asej.2020.09.015

Bappa Das, Sujeet Desai, Amrita Daripa, Gurav Chandrakant Anand, Uttam Kumar, Dhiraj Khalkho, Velumani Thangavel, Nirmal Kumar, Gangalakunta P. Obi Reddy and Parveen Kumar (2023). Land degradation vulnerability mapping in a west coast river basin of India using analytical hierarchy process combined machine learning models. Environ. Sci. Pollut. Res., pp. 1-16. https://doi.org/10.1007/s11356-023-28276-4

Ben-Dor, E., Inbar, Y. and Chen, Y. (1997). The reflectance spectra of organic matter in the visible near-infrared and short wave infrared region (400–2500 nm) during a controlled decomposition process. *Rem. Sens. Environ.*, v.*61*(1), pp.1-15. https://doi.org/10.1016/s0034-4257(96)00120-4

Bhattacharyya, T., Pal, D. and Deshpande, S.M. (1993). Genesis and transformation of minerals in the formation of red (Alfisols) and black (Inceptisols and Vertisols) soils on Deccan basalt in the Western Ghats, India. Jour. Soil Sci., v.44(1), pp.159–171. https://doi.org/10.1111/j.1365-2389.1993.tb00442.x

Bhattacharyya, T., Pal, D. and Srivastava, P.K. (1999). Role of zeolites in persistence of high altitude ferruginous Alfisols of the humid tropical Western Ghats, India. Geoderma, v.90(3-4), pp.263-276. https://doi.org/10.1016/s0016-7061(98)00122-0

Cai, Y., Lin, H. and Zhang, M. (2019). Mapping paddy rice by the object-based random forest method using time series Sentinel-1/Sentinel-2 data. Advanc. Space Res., v.64(11), pp.2233–2244. https://doi.org/10.1016/j.asr.2019.08.042

Castaldi, F., Hueni, A., Chabrillat, S., Ward, K., Buttafuoco, G., Bomans, B., Vreys, K., Brell, M. and Van Wesemael, B. (2019). Evaluating the capability of the Sentinel 2 data for soil organic carbon prediction in croplands. Isprs Jour. Photogramm. Rem. Sens., v. *147*, pp.267–282. https://doi.org/10.1016/j.isprsjprs.2018.11.026

Cowie, A., Orr, B. J., Sanchez, V., Chasek, P. S., Crossman, N. D., Erlewein, A., Louwagie, G., Maron, M., Metternicht, G., Minelli, S., Tengberg, A. E., Walter, S. and Welton, S. (2018). Land in balance: The scientific conceptual framework for Land Degradation Neutrality. Environment. Sci. Policy, v. 79, pp.25–35. https://doi.org/10.1016/j.envsci.2017.10.011

Cox, K. G. and Hawkesworth, C.J. (1985). Geochemical Stratigraphy of the Deccan Traps at Mahabaleshwar, Western Ghats, India, with Implications for Open System Magmatic Processes. Jour. Petrol., v.26(2), pp.355–377. https://doi.org/10.1093/petrology/26.2.355

Dobbs, C., Robinson, A.P. and Kendal, D. (2017). Assessing the drivers shaping global patterns of urban vegetation landscape structure. Sci. Total Environ., v. 592, pp.171–177. https://doi.org/10.1016/j.scitotenv.2017.03.058

DRM (2022). District Resource map of Raigad district. Geological Survey of India, Central Region

Fleskens, L. and Stringer, L.C. (2014). Land management and policy responses to mitigate desertification and land degradation. Land Degrad. Develop., v. 25(1), pp. 1–4. https://doi.org/10.1002/ldr.2272

Forkel, M., Carvalhais, N., Verbesselt, J., Mahecha, M.D., Neigh, C.S. and Reichstein, M. (2013). Trend Change Detection in NDVI Time Series: Effects of Inter-Annual Variability and Methodology. Rem. Sens., v.5(5), pp.2113–2144. https://doi.org/10.3390/rs5052113

Godbole S.M., Rana R.S. and Natu S.R. (1996). Lava stratigraphy of Deccan Basalts of western Maharashtra; *In*: Deccan Basalts (*Eds.*) Deshmukh, S.S. and Nair, K.K.K., Gond. Geol. Soc. Spec. Publ., v. 2, pp. 125–134.

Grelle, G., Soriano, M. L., Revellino, P., Guerriero, L., Anderson, M. W., Diambra, A., Fiorillo, F., Esposito, L., Diodato, N. and Guadagno, F.M. (2014). Space–time prediction of rainfall-induced shallow landslides through a combined probabilistic/deterministic approach, optimized for initial water table conditions. Bull. Engineer. Geol. Environ., v. 73(3), pp. 877-890. https://doi.org/10.1007/s10064-013-0546-8

CGWB (2013). Government of India, Ministry of Water Resources, Central Ground Water Board, Ground Water Information of Raigarh District, Maharashtra, 1807/DBR/2013.

Gurav Chandrakant, Babar Md, Patil Yogita, Patil Abijeet and Patode, H.S. (2017). Application of Remote Sensing, Geology And Geomorphological Studies for Mass Wasting Zone analysis in Jotiba-Panhala Hill Range area, Kolhapur District, Maharashtra, India. IOSR Jour. Appl. Geol. Geophys. (IOSR-JAGG), v.5, pp. 29-37.

Horton, R.E. (1945). Erosional development of streams and their drainage basins; hydrophysical approach to quantitative morphology. GSA Bull. GeoSci. World. https://doi.org/10.1130/0016-7606(1945)56

Kale, V.S. and Najaguru, S.N. (1988). Morphology and denudation chronology of the Coastal and Upland river basins of western Deccan Trappean landscape (India): a collation. Zeitschrift Fur Geomorphologie, v.32(3), pp.311–327. https://doi.org/10.1127/zfg/32/1988/311

Kosmas, C., Danalatos, N. and Gerontidis, S. (2000). The effect of land parameters on vegetation performance and degree of erosion under Mediterranean conditions. Catena, v.40(1), pp.3–17. https://doi.org/10.1016/s0341-8162(99)00061-2

Mahoney, J.J. (1988). Deccan Traps. *In*: Petrology and Structural Geology, pp. 151–194. Springer Nature (Netherlands). https://doi.org/10.1007/978-94-015-7805-9_5

Maji, A.K., Reddy, G.P.O. and Sarkar, D. (2010). Degraded and Wastelands of India, Status, and Spatial Distribution; ICAR and NAAS Publication: Cochin, India, pp. 1–158.

Mikoš, M., Jošt, D. and Petkovšek, G. 2006. Rainfall and runoff erosivity in the alpine climate of north Slovenia: a comparison of different estimation methods. Hydrol. Sci. Jour.- Jour. Sci. Hydrologiques, v.51(1), pp.115–126. https://doi.org/10.1623/hysj.51.1.115

Mzuri, R.T., Mustafa, Y.T. and Omar, A.A. (2021). Land degradation assessment using AHP and GIS-based modelling in Duhok District, Kurdistan Region, Iraq. Geocarto Int., pp.1–19. https:// doi.org/10.1080/10106049.2021.1987534

NBSS&LUP (1996). Maharashtra Soils. Nagpur, India: National Bureau of Soil Survey and Land Use Planning.

Nachtergaele, F., Biancalani, R., Bunning, S., George, H. and FAO of the U.N. (2010). Land Degradation Assessment: the LADA approach. In: 19th World Congress of Soil Science, Soil Solutions for a Changing World.

Nocita, M., Stevens, A., Van Wesemael, B., Aitkenhead, M., Bachmann, M. F., Barthès, B., Ben-Dor, E., Brown, D., Clairotte, M., Csorba, Á., Dardenne, P., Demattê, J. A. M., Genot, V., Guerrero, C., Knadel, M., Montanarella, L., Noon, C., Ramirez-Lopez, L., Robertson, J., Wetterlind, J. (2015). Soil Spectroscopy: An Alternative to Wet Chemistry for Soil Monitoring. *In*: Advances in Agronomy, pp. 139–159, Elsevier BV. https://doi.org/10.1016/bs.agron.2015.02.002

Pal, I. and Al-Tabbaa, A. (2009). Trends in seasonal precipitation extremes – An indicator of 'climate change' in Kerala, India. Jour. Hydrol., v.367(1–2), pp. 62–69. https://doi.org/10.1016/j.jhydrol.2008.12.025

Reddy, G.M., Kumar, N.T. and Singh, S.K. (2018). Remote sensing and GIS in mapping and monitoring of land degradation. *In*; Geotechnologies and the environment, pp. 401–424, Springer International Publishing. https://doi.org/10.1007/978-3-319-78711-4_20

Reddy, S.B. (2003). Estimation of watershed runoff using artificial neural networks. Ph.D Thesis in Agric. Engg. (unpubl.). Post Graduate School, IARI, New Delhi.

Saaty, T.L. (1980). The analytic hierarchy process: planning, priority setting, resource allocation. https://ci.nii.ac.jp/ncid/BA33072871

Saaty, T.L. and Vargas, L.G. (2012). Models, Methods, Concepts and Applications of the Analytic Hierarchy Process. *In*: International series in management science/operations research. https://doi.org/10.1007/978-1-4614-3597-6

Samal, D.R., Gedam, S.S. and Nagarajan, R. (2015). GIS based drainage morphometry and its influence on hydrology in parts of Western Ghats region, Maharashtra, India. Geocarto Internat., v.30(7), pp.755–778. https://doi.org/10.1080/10106049.2014.978903

Samal, D.R., Mendiratta, P. and Gedam, S.S. (2014). Object-based, land use change detection: Lessons from change matrix. Proceedings of the national conference on application of geoinformatics in rural, urban and climatic studies (Geomatrix'14). India: Indian Institute of Technology Bombay.

Sandeep, P., Reddy, G.M., Jegankumar, R. and Kumar, K.S. (2020). Modeling and Assessment of Land Degradation Vulnerability in Semi-arid Ecosystem of Southern India Using Temporal Satellite Data, AHP and GIS. Environment. Model. Assess., v.26(2), pp.143–154. https://doi.org/10.1007/s10666-020-09739-1

Sar, N., Chatterjee, S. and Adhikari, M.D. (2015). Integrated remote sensing and GIS based spatial modelling through analytical hierarchy process (AHP) for water logging hazard, vulnerability and risk assessment in Keleghai river basin, India. Model. Earth Syst. Environ., pp. 1–31.

Schmidt, S.A., Alewell, C., Panagos, P. and Meusburger, K. (2016). Regionalization of monthly rainfall erosivity patterns in Switzerland. Hydrol. Earth Syst. Sci., v.20(10), pp.4359–4373. https://doi.org/10.5194/hess-20-4359-2016

Schumm, S.A. (1963). Sinuosity of alluvial rivers on the Great Plains. Geol. Soc. Am. Bull., v.74(9), pp.1089. https://doi.org/10.1130/0016-7606(1963)74

Schumm, S.A., and Hadley, R.F. (1961). Progress in the application of landform analysis in studies of semiarid erosion. U.S. Geol. Surv. Circ., v.437, 14p.

Shekhar, S. and Pandey, A.C. (2014). Delineation of groundwater potential zone in hard rock terrain of India using remote sensing, geographical information system (GIS) and analytic hierarchy process (AHP) techniques. Geocarto Internat., v.30(4), pp.402–421. https://doi.org/10.1080/10106049.2014.894584

Sujatha, G., Dwivedi, R., Sreenivas, K. and Venkataratnam, L. (2000). Mapping and monitoring of degraded lands in part of Jaunpur district of Uttar Pradesh using temporal spaceborne multispectral data. Internat. Jour. Rem. Sens., v.21(3), pp.519–531. https://doi.org/10.1080/014311600210722

Torabi Haghighi A, Darabi H, Karimidastenaei Z *et al.* (2021). Land degradation risk mapping using topographic, human-induced, and geo-environmental variables and machine learning algorithms, for the Pole-Doab watershed. Iran Environ. Earth Sci., v.80, 1. https://doi.org/ 10. 1007/ s12665- 020- 09327-2

Wischmeier, W.H. and Smith, D.L. (1958). Rainfall energy and its relationship to soil loss. Transactions, v.39(2), pp.285. https://doi.org/10.1029/tr039i002p00285

Wischmeier, W. and Smith, D. (1978). Predicting rainfall erosion losses: a guide to conservation planning. Agricultural Handbook No. 537. U.S. Department of Agriculture, Washington, D.C, USA.

Yang, L., He, X., Shen, F., Zhou, C., Zhu, A., Gao, B., Chen, Z. and Li, M. (2020). Improving prediction of soil organic carbon content in croplands using phenological parameters extracted from NDVI time series data. Soil Till. Res., v. 196, 104465. https://doi.org/10.1016/j.still.2019.104465

Zhang, Y., Chen, Z., Zhu, B., Luo, X., Guan, Y., Guo, S. S. and Nie, Y. (2008). Land desertification monitoring and assessment in Yulin of Northwest China using remote sensing and geographic information systems (GIS). Environment. Monitor. Assess., v.147(1–3), pp.327–337. https://doi.org/10.1007/s10661-007-0124-2